

### Drawings

The Examiner strongly advises Applicants to use the correct shading in the drawings, but makes no objection or rejection to them. Upon indication of allowable subject matter, Applicants may correct the shading in the drawings.

### Claim Rejections - 35 U.S.C. § 103

The Examiner rejected claims 1-55 and 64-67 under §103(a) as being unpatentable over US Patent 5,212,496 to Badesha et al. (hereinafter Badesha) in view of US Patent 5,124,716 to Roy et al. (hereinafter Roy). Applicants respectfully traverse this rejection because the references fail to establish *prima facie* obviousness in that they do not teach or suggest every element as set forth in Applicants' claims.

First, Applicants' arguments as set forth in the Amendment filed July 1, 2002, on pages 2-5, are still pertinent and, therefore, are incorporated herein by reference.

Second, the Examiner asserts that Applicants have not presented any "evidence, i.e. 37 CFR 1.132" that the materials used by the prior art do not have a compressive stress as compared to the materials used by the Applicants.<sup>1</sup> However, because the Examiner has failed even to establish *prima facie* obviousness, Applicants are under no obligation to present any evidence of non-obviousness. Specifically, because the Examiner has not presented any teaching or suggestion of a compression film having a compressive stress, as claimed, Applicants are under no obligation to present evidence that the references do not teach or suggest such an element. Nonetheless, Applicants have presented—in the Amendment filed on January 10, 2002—articles explaining that not all materials include a compressive stress. As further evidence that not all films include a compressive stress, Applicants have submitted herewith an article entitled "Stresses in Pt/Pb(ZrTi)O<sub>3</sub>/Pt thin-film stacks for integrated ferroelectric capacitors", by G.A.C.M. Spierings et al., Journal of Applied Physics, vol. 78 (3), August 1, 1995, pp. 1926-1933 (hereinafter Spierings).

---

<sup>1</sup> September 11 Office Action at page 2, item number 4.

Spierings teaches that several different stresses, such as intrinsic stress and thermal stress, can be present in a thin film. Spierings goes on to teach that the magnitude of the intrinsic stress is largely determined by the deposition conditions—i.e., how the film was made—and change upon annealing. See, for example, page 1927, right column, 1<sup>st</sup> full paragraph to page 1928, end of left column. Additionally, with respect to the platinum bottom electrode, Spierings specifically teaches that the “stress in a sputtered metal film can be varied over a wide range, from tensile to compressive, by modifying sputter conditions such as pressure and power.”<sup>2</sup> Further, with respect to the stresses in the PZT film, Spierings teaches that a first PZT layer is compressive, whereas two subsequent layers are increasingly tensile.<sup>3</sup> Moreover, Spierings teaches that the stresses in each of the electrodes and PZT film changed from compressive to tensile, or vice versa, upon annealing. See, for example, Table III, and the paragraph bridging pages 1930-1931. Also, see section VI. Discussion and Conclusions on pages 1932-1933.

In light of the above, Applicants have shown that it is readily known within the skill of the art that not all materials include a compressive stress, and that the stress profile of a material depends upon how it was made, and to what annealing treatments it was subjected. Accordingly, the Examiner’s assertion that Badesha includes a compressive stress is in error. That is, as noted in the first argument, above, Badesha does not use the terms “compressive” or “compression” at all, and further does not disclose any particular process by which his films are made. Therefore, Badesha contains no teaching or suggestion of a compression film having a compressive stress, as claimed.

In contrast to that in the references cited by the Examiner, the present invention is characterized by a feature in which a film having a compressive stress is removed at a certain location to cancel (or release) a residual stress to thereby avoid the undesired deformation of the

---

<sup>2</sup> Spierings at page 1928, right column, paragraph carrying over to page 1929.

<sup>3</sup> Spierings at page 1929, right column, last paragraph, carrying over to page 1930.

film and improve the performance of the piezoelectric element. See, for example, the second paragraph of page 15 in the present specification.

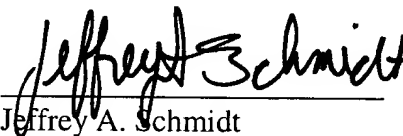
For at least any of the above reasons, the Examiner's rejection based on Badesha and Roy is believed to be in error, and should be withdrawn.

**Conclusion**

In view of the above, reconsideration and allowance of this application are now believed to be in order, and such actions are hereby solicited. If any points remain in issue which the Examiner feels may be best resolved through a personal or telephone interview, the Examiner is kindly requested to contact the undersigned at the telephone number listed below.

The USPTO is directed and authorized to charge all required fees, except for the Issue Fee and the Publication Fee, to Deposit Account No. 19-4880. Please also credit any overpayments to said Deposit Account.

Respectfully submitted,

  
\_\_\_\_\_  
Jeffrey A. Schmidt

Registration No. 41,574

SUGHRUE MION, PLLC  
Telephone: (202) 293-7060  
Facsimile: (202) 293-7860

WASHINGTON OFFICE



23373

PATENT TRADEMARK OFFICE

Date: March 10, 2003

**This Page Is Inserted by IFW Operations  
and is not a part of the Official Record**

## **BEST AVAILABLE IMAGES**

**Defective images within this document are accurate representations of the original documents submitted by the applicant.**

**Defects in the images may include (but are not limited to):**

- **BLACK BORDERS**
- **TEXT CUT OFF AT TOP, BOTTOM OR SIDES**
- **FADED TEXT**
- **ILLEGIBLE TEXT**
- **SKEWED/SLANTED IMAGES**
- **COLORED PHOTOS**
- **BLACK OR VERY BLACK AND WHITE DARK PHOTOS**
- **GRAY SCALE DOCUMENTS**

**IMAGES ARE BEST AVAILABLE COPY.**

**As rescanning documents *will not* correct images,  
please do not report the images to the  
Image Problem Mailbox.**

# Stresses in $\text{Pt}/\text{Pb}(\text{Zr},\text{Ti})\text{O}_3/\text{Pt}$ thin-film stacks for integrated ferroelectric capacitors

G. A. C. M. Spierings,<sup>a)</sup> G. J. M. Dormans, W. G. J. Moors, M. J. E. Ulenlaers, and P. K. Larsen

<sup>a)</sup>Philips Research Laboratories, Prof. Holstlaan 4, 5656-AA Eindhoven, The Netherlands

(Received 19 September 1994; accepted for publication 11 April 1995)

A study of the stresses in a ferroelectric capacitor stack deposited on an oxidized silicon substrate is presented. The capacitor stack was prepared with sputtered Pt bottom and top electrodes and a ferroelectric film of composition  $\text{PbZr}_x\text{Ti}_{1-x}\text{O}_3$  (PZT) with  $x \approx 0.5$  which was deposited using a modified sol-gel technique. The stresses were determined by the changes in the radius of curvature of the wafer following the deposition steps, during and after annealing treatments, and after etching steps in which the top electrode, the PZT film, and the bottom electrode were successively removed. The largest stress effects are found in the Pt electrodes which are deposited under conditions giving an intrinsic compressive stress. An annealing treatment exceeding 500 °C changed the stress of the bottom electrode from  $\approx -750$  MPa (compressive) to a large tensile stress ( $\approx 1$  GPa). This stress is largely thermal and is caused by the differences in thermal-expansion coefficients of the Pt film and the Si substrate. The stress of the PZT film is numerically relatively small (below  $\approx 200$  MPa) and it is found to be of both thermal and intrinsic origin. The deposition and annealing of the top electrode has a profound influence on the stress of the PZT film as well as on the electrical properties. The stress behavior of the as-deposited PZT film shows a poling direction mainly in the plane of the substrate. An annealing of the complete capacitor stack changes the poling direction of the ferroelectric film to be perpendicular to the substrate. This explains the observed electrical switching properties of as-prepared as well as annealed ferroelectric capacitors. © 1995 American Institute of Physics.

圧縮応力で、 $P_r$ が低く、 $E_c$ が増加する。

## I. INTRODUCTION

The presence of stress in a ferroelectric thin film can be expected to influence the electrical properties of an integrated ferroelectric capacitor.<sup>1</sup> It is well established that stresses in  $\text{Pb}(\text{Zr},\text{Ti})\text{O}_3$  ceramics influence properties such as dielectric permittivity,  $\tan(\delta)$ , and piezoelectric coefficients.<sup>2</sup> The effects are most pronounced for compressive stresses applied parallel to the polar axis. PZT can react to an applied stress by 90° reorientation for the tetragonal and 109° and 71° reorientation for the rhombohedral phase.<sup>1</sup> This indicates the possibility of stress-induced effects in the switching behavior of a PZT film. Furthermore, excessive tensile stresses in the films may result in film cracking and edge delamination, and compressive stresses can result in buckling of the film.<sup>3</sup>

Stresses in ferroelectric thin films and their effects on some properties have been subjects of recent investigations. Desu showed that for  $\text{BaTiO}_3$  films the hysteresis curve deteriorates (remnant polarization  $P_r$  decreases while the coercive field  $E_c$  increases) when the film is compressively stressed.<sup>4</sup> Tuttle *et al.* found similar effects for PZT films. The compressive PZT films deposited on sapphire exhibit superior ferroelectric properties as compared to tensile films deposited on silicon substrates.<sup>5</sup> Tuttle *et al.* suggested that the stress conditions at the Curie point determine the crystallite/domain orientation within the PZT film and consequently the ferroelectric behavior.

圧縮応力では、 $P_r$ が低く、 $E_c$ が増加する。

<sup>a)</sup>Electronic mail: spiering@prl.philips.nl

In this paper the evolution of stress during processing of a ferroelectric capacitor prepared with Pt bottom and top electrodes and sol-gel  $\text{PbZr}_x\text{Ti}_{1-x}\text{O}_3$  ( $x \approx 0.5$ ) film on an oxidized Si substrate is reported. The materials and processing conditions used in this investigation are the result of an extensive study directed toward optimizing the properties of the ferroelectric capacitor for nonvolatile memory applications.<sup>6-8</sup>

First, the stress after deposition and after annealing treatments is determined for each film. Second, the influence of interactions between the different layers of the capacitor is described on the basis of stress data obtained from a step-by-step removal of the films in the completed capacitor stack. Finally, the effects of stresses in the PZT film prior to and after the top electrode annealing on the switching behavior of the capacitor are discussed.

## II. EXPERIMENTAL METHODS

### A. Thin-film deposition and etching

The bottom electrodes, which consisted of a 4 nm adhesion-promoting Ti layer and a 70 nm Pt film, were sputter-deposited on 100 mm diameter oxidized silicon wafers using a Nordiko NS2050 sputter system without substrate heating. However, during deposition some heating of the wafer to about 60 °C is unavoidable. The properties of these electrodes in relation to the PZT deposited on top of them have been described in more detail in Ref. 6.

PZT films with compositions near the morphotropic phase boundary ( $x \approx 0.5$ ) were deposited by a modified sol-gel technique. The process consisted of three spin-coated

圧縮応力では、 $P_r$ が低く、 $E_c$ が増加する。

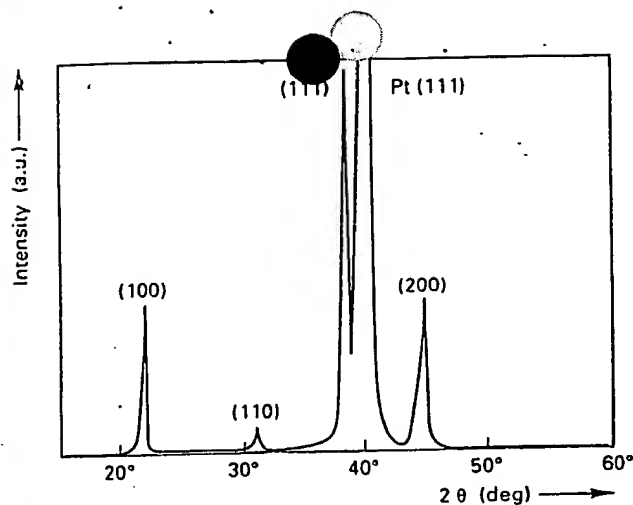


FIG. 1. X-ray-diffraction pattern of PZT used in this investigation.

layers with thicknesses of 90, 65, and 65 nm, respectively. After deposition of each layer a bakeout treatment was applied. This consisted of a 30 min heat treatment in  $N_2/O_2$  at 550 °C for the first layer and at 600 °C for the other two layers. The deposition was completed with a final annealing (650 °C,  $N_2/O_2$ , 30 min). The x-ray-diffraction pattern (Fig. 1) shows that in the PZT film all crystallite orientations are present but that there is a preferential orientation in the (111) and to a lesser degree in the (100) direction. The composition is too close to the morphotropic phase boundary to show any splitting of the (100) or (200) peaks. It was pointed out in Ref. 7 that the splitting of (*h*00) and (00*h*) lines in the diffraction pattern of tetragonal PZT close to the morphotropic phase boundary (where the splitting becomes small) is obstructed in fine grained films due to the broadening of the diffraction lines.

The top electrode (70 nm Pt+7 nm Ti) was sputter-deposited with the same conditions as used for the bottom electrode. The Pt film was etched by ion-beam milling<sup>9</sup> and the PZT film was wet chemically etched.

## B. Stress measurements

Stress in a thin film deposited on a circular substrate results in a spherical warpage of the substrate. A commercial stress analyzer (Tencor FLX-2900) was used to measure this warpage with a laser-reflection system. This analyzer can measure the warpage of the wafer *in situ* during heating to 900 °C. The total stress  $\sigma$  in the film can be calculated from the difference in the radii of curvature before ( $R_0$ ) and after ( $R$ ) a particular processing step (e.g., deposition or annealing), using the Stoney formula<sup>10</sup>

$$\sigma = \frac{E_s}{6(1-\nu_s)} \frac{t_s^2}{t_f} \left( \frac{1}{R} - \frac{1}{R_0} \right), \quad (1)$$

where  $t_f$  is the film thickness and  $E_s$ ,  $\nu_s$ , and  $t_s$  are the elastic modulus, Poisson ratio, and thickness of the substrate, respectively. Negative values for  $\sigma$  indicate a compressive stress and positive ones a tensile stress. Two types of measurements were used in this investigation. First of all, the

TABLE I. Young's moduli ( $E_s$ ) and Poisson ratio ( $\nu_s$ ) of Pt (see Ref. 11), unpoled polycrystalline PZT (see Ref. 13), and Si (see Ref. 12).

	$E_s$ (GPa)	$\nu_s$
Pt	170	0.39
PZT	72	0.30
Si	130	0.28

stress was measured at room temperature after a specific processing treatment as a function of the processing parameters. Second, *in situ* stress measurements were carried out with the stress analyzer while the film underwent a thermal cycling process. The latter had to be done in  $N_2$ , since stress measurements in oxygen-containing atmospheres were not possible at temperatures above a few hundred degrees Celsius.

The application of Eq. (1) for calculating the stress in a particular film requires that the substrate and any previously deposited films not be influenced during the deposition of the film under study. Possible effects in the substrate and underlying films include recrystallization, interdiffusion, chemical reaction, and plastic deformation processes. Such processes are likely to occur during an anneal treatment in any of the films in a stack. In order to isolate the effects in one particular film without interference from changes in the stress-related conditions within any of the other films, the stress is measured before and after removal of the film, e.g., by etching. In this way the effects of an anneal treatment in a particular film can be determined separately from changes in other films. The total stress in a multiple stack is the sum of the stresses in each film.

In general several different stresses contribute to the total stress;<sup>3</sup> the intrinsic stress  $\sigma_{int}$  and the thermal stress  $\sigma_{th}$  are the most relevant ones for this investigation. The intrinsic (or growth) stress is the result of the accumulation of structural imperfections that are built into the film during the deposition process. Its magnitude is largely determined by the thin-film deposition conditions. Generally, when films are annealed the intrinsic stresses are reduced by interdiffusion, recrystallization, and grain growth processes. On subsequent cooling (to room temperature) a thermal stress is introduced. The thermal stress originates from the difference in thermal expansion between the substrate and the thin-film material over the cooling range from an annealing temperature  $T_{anneal}$  to a temperature  $T_0$ . It is given by

$$\sigma_{th} = \frac{E_f}{1-\nu_f} \int_{T_{anneal}}^{T_0} (\alpha_f - \alpha_s) dT. \quad (2)$$

$E_f$  and  $\nu_f$  are the Young's modulus and the Poisson ratio of the film material. These properties are given in Table I.  $\alpha_f$  and  $\alpha_s$  are the thermal-expansion coefficients of the film and substrate, respectively. For this study the thermal-expansion coefficient of Pt and Si given in Refs. 11 and 12, respectively, are used. For PZT we used the data reported by Cook, Jr., Berlincourt, and Scholz for bulk material with composition  $PbZr_{0.52}Ti_{0.48}O_3$  doped with 1%  $Nb_2O_5$ .<sup>13</sup> Figure 2 shows the thermal-expansion coefficients for unpoled PZT ( $\alpha$ ), for poled PZT perpendicular ( $\alpha_1$ ) to the poling direction,

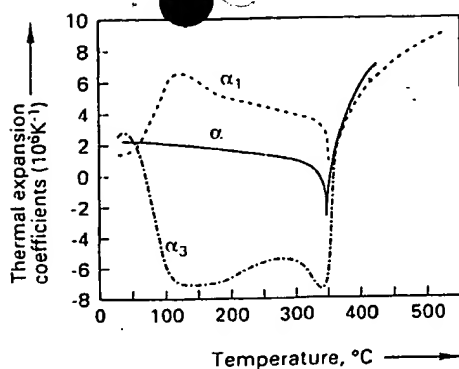


FIG. 2. Thermal-expansion coefficients for  $\text{PbZr}_{0.52}\text{Ti}_{0.48}\text{O}_3$  with 1%  $\text{Nb}_2\text{O}_5$  ceramics for unpoled ( $\alpha$ ) and poled material ( $\alpha_1, \alpha_3$ ) (see Ref. 13). The latter shows a strong asymmetry for the directions parallel ( $\alpha_1$ ) and perpendicular ( $\alpha_3$ ) to the poling direction.

and poled PZT parallel ( $\alpha_3$ ) to the poling direction. We will use these data in Eq. (2) to calculate the thermal stresses within the Pt and PZT films deposited on a Si substrate.

In addition to "bulk" film stresses, interfacial stresses may also be present. This is the result of the work required to elastically deform a unit area of interface and is relatively small. For instance, in  $\text{Au}/\text{Al}_2\text{O}_3$  multilayers interface stresses only contribute significantly to the total film stress in case the alternating Au and  $\text{Al}_2\text{O}_3$  films have thicknesses smaller than 10 nm.<sup>14</sup> Consequently, interfacial stress will not be discussed further in this paper.

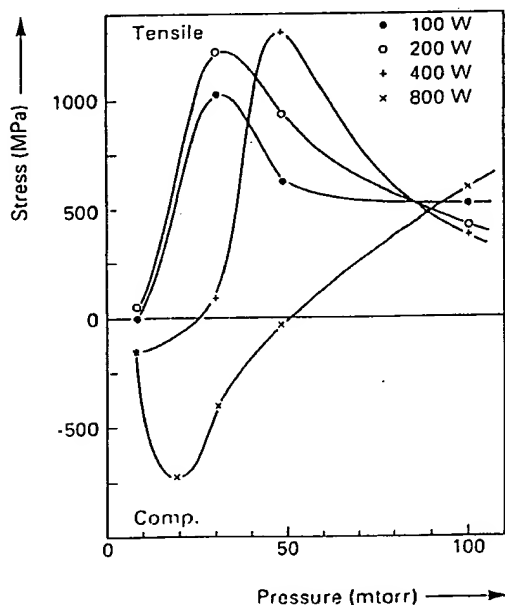


FIG. 3. The stress of 4 nm Ti+70 nm Pt films deposited on 100 nm oxidized silicon wafers as a function of pressure in the deposition chamber for four power settings.

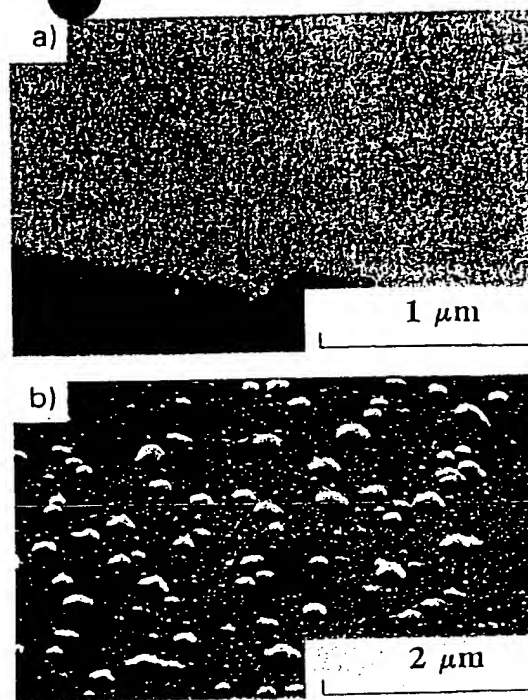


FIG. 4. Scanning electron micrograph of (a) an unannealed bottom electrode showing no texture and (b) an annealed bottom electrode showing small hillocks. The film thickness was 4 nm Ti+70 nm Pt and the anneal temperature was 700 °C.

### C. Pulse measurements

The measurements of the switched and nonswitched polarization of capacitors prepared from the  $\text{P}/\text{PZT}/\text{Pt}$  stacks were performed following the methods described in Ref. 15. The size of these capacitors was  $2000 \mu\text{m}^2$ . The processing of the capacitors has been described elsewhere.<sup>8</sup>

## III. STRESS EVOLUTION DURING PROCESSING

### A. Stresses in the Pt bottom electrode

The stress in a sputtered metal film can be varied over a wide range, from tensile to compressive, by modifying sputter conditions such as pressure and power.<sup>3</sup> This typical behavior is also observed for the 4 nm Ti+70 nm Pt bottom electrode. Figure 3 shows the stress for films deposited with variations in the pressure within the sputter chamber for different power settings of the machine. The pressure at which the compressive-tensile transition occurs increases with the applied power. A power of 800 W and an Ar pressure of 20 mTorr are used as standard conditions for platinum deposition in this work. Under these conditions highly compressive bottom electrodes are deposited with  $\sigma = -700$  to  $-750$  MPa. For the deposition of PZT by the sol-gel technique applied here it is essential to anneal the bottom electrode at temperatures above 600 °C prior to the PZT deposition. The hillocks which are formed at the surface of the platinum film (Fig. 4) act as nuclei for the crystallization of the perovskite PZT phase and lead to a fine grained PZT film without any

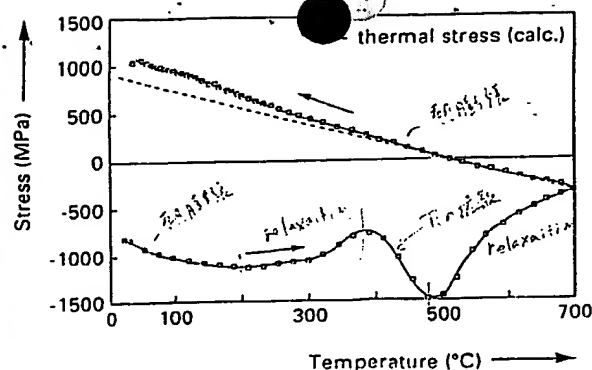


FIG. 5. Stress in a 4 nm Ti+70 nm Pt film on an oxidized silicon wafer during a thermal cycle in  $N_2$ . Also shown is the theoretical thermal stress (dashed broken line) calculated from the thermal-expansion coefficients of Si (see Ref. 12) and Pt (see Ref. 10).

second phases.<sup>6</sup> Both the stress evolution during thermal cycling in nitrogen and the stress level after a furnace annealing in  $N_2/O_2$  were investigated.

### 1. Stress development during thermal cycling

The platinized wafer was heated in the furnace of the stress analyzer at a rate of 15 °C/min in a nitrogen atmosphere from 25 °C to a temperature of 700 °C and subsequently cooled to room temperature. During this thermal cycle the stress was determined at regular time intervals. The results are shown in Fig. 5.

Initially upon heating the compressive strength increases almost linearly due to a larger thermal expansion of platinum compared to the silicon wafer. Above 200 °C some stress relaxation starts, but between 370 and 500 °C the compressive stress increases, presumably due to the diffusion of a part of the Ti into the Pt film.<sup>16</sup> Above 500 °C a stress relaxation process is observed, caused by recrystallization processes within the Pt film resulting in a much stronger Pt(200) XRD reflection;<sup>6</sup> this occurs in combination with the formation of small hillocks as illustrated in Fig. 4. The compressive stress decreases to a relatively small value. Some additional stress relaxation occurs when the wafer is kept for a longer time at 700 °C. During cooling of the wafer to room temperature a large tensile stress develops. This is due to the much larger thermal expansion of platinum as compared to silicon substrate. The thermal stress calculated using Eq. (2) (dotted line in Fig. 5) agrees very well with the experimental stress data obtained during cooling. A completed thermal cycle changes the stress from a 700 MPa compressive stress which is mostly intrinsic in nature to a thermal tensile stress of about 1000 MPa. Repeating this heating cycle again gives the upper curve of Fig. 5 which indicates a stable stress situation in the Pt electrode after annealing.

### 2. Stress after an $N_2/O_2$ anneal treatment

A standard treatment of the bottom electrode prior to the PZT deposition consists of an annealing of 30 min in  $N_2/O_2$ . The resulting stress for different anneal temperatures is shown in Fig. 6. After an annealing at above 600 °C the

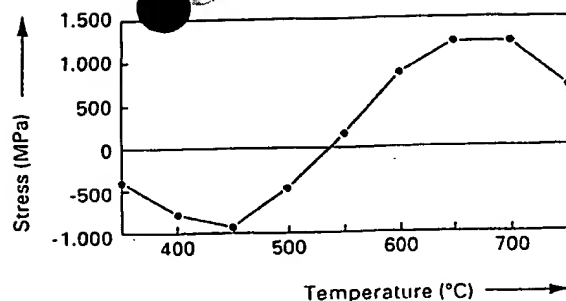


FIG. 6. The room-temperature stress of a 4 nm Ti+70 nm Pt bottom electrode after annealing for 30 min in  $N_2/O_2$  for various anneal temperatures.

stress is thermal in nature and the Pt film is also covered with small hillocks. The thin Ti film is oxidized and a small part of it has diffused to the surface.<sup>6</sup> Nevertheless, a sharp interface between the  $TiO_2$  and the Pt film is still observed. After an annealing at 650 °C, the standard for our PZT deposition method, a stress of 950 MPa tensile is found, which is very similar to the value found after the thermal cycling in  $N_2$ . Electrodes annealed at lower temperatures (450 and 550 °C with  $\sigma = -660$  and 166 MPa, respectively) were also used for PZT deposition. This allows the investigation of effects of subsequent PZT and top electrode processing on the stress in the not fully annealed bottom electrode (see Sec. IV A).

### B. Stresses in the PZT film

The PZT film was deposited using the standard procedure described above. In this section only results for bottom electrodes annealed at 650 °C will be treated. The curvatures of the wafer were measured after each spin-coating step (including the bakeout) and after the final annealing. The stress in each layer was calculated from the curvature using Eq. (1). The results are given in Table II. The stress levels in the PZT film are much smaller than those in the Pt electrode. This partly reflects a much smaller difference in thermal-expansion coefficients between the PZT film and the substrate than between the Pt film and the substrate.

The first PZT layer deposited on the Pt film is compressive and the two subsequent layers deposited on PZT itself are increasingly tensile. This difference indicates that the level of the intrinsic stress in the PZT depends on the underlying material on which it is deposited. The combined stress in the three-layer PZT film amounts to 18 MPa tensile (Table

TABLE II. The stress at room temperature after deposition and bakeout of each of the three PZT layers as well as integrated over the complete stack and after the final annealing.

	Film thickness (nm)	Stress (MPa)
PZT layer 1	90	-128
PZT layer 2	65	51
PZT layer 3	65	191
PZT total	220	18
PZT annealed	220	113



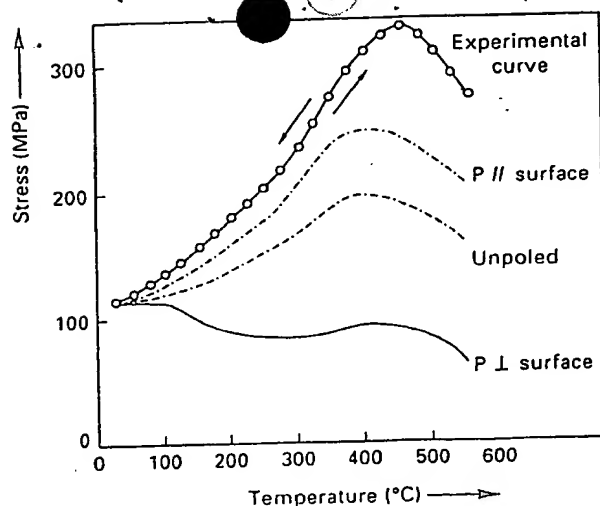


FIG. 7. Stress in a 220 nm PZT film prepared by sol gel as a function of temperature during thermal cycling from 25 to 550 °C. The experimentally determined stress is compared with the thermal stress calculated from the thermal-expansion coefficient of the PZT film (see Ref. 13) for three cases: (a) unpoled polycrystalline PZT (-----), (b) poled polycrystalline PZT with the polarization directed parallel to the plane of the film (-----), and (c) the same with the polarization directed perpendicular to the surface (—).

II). An anneal treatment at 650 °C increases the level of tensile stress to 113 MPa. The stress development of each of the separate spin-coated PZT films was not investigated separately. In the rest of this paper we treat the stress as being homogeneous and present over the whole PZT film.

The stress in the annealed PZT film as a function of temperature was determined by the thermal cycling from 25 to 550 °C of a film in nitrogen. The results of these measurements are shown in Fig. 7. A maximum stress is observed at about 450 °C. By repeating the thermal cycling the same curve is obtained, which indicates that the stress is thermal in nature and is caused by the differences in thermal-expansion coefficients between film and substrate. The shape of the curve can be understood on the basis of the thermal-expansion data for bulk PZT ( $\alpha_{\text{PZT}}$ ) as measured by Cook, Jr. *et al.* both for both unpoled and poled material<sup>12</sup> and as shown in Fig. 2.

Our films do show a preferential (111) and (100) orientation, but all crystallite orientations are essentially present. Therefore a qualitative comparison with the randomly oriented bulk PZT material is possible. As shown in Fig. 2 for unpoled material,  $\alpha_{\text{PZT}}$  has a large temperature dependence. Below the Curie temperature ( $T_c$ ) it is smaller than that of the substrate material silicon, which has a thermal-expansion coefficient that gradually increases from  $2.5 \times 10^{-6}$  at 25 °C to  $4.1 \times 10^{-6}$  at 600 °C.<sup>13</sup> At higher temperatures the thermal-expansion coefficient of PZT exceeds that of silicon. The thermal-expansion coefficient becomes very anisotropic after poling. For the direction parallel to the polarization the thermal expansion coefficient ( $\alpha_3$ ) has a large negative value, while for the direction perpendicular to the polarization a positive thermal-expansion coefficient ( $\alpha_1$ ) not very different from that of Si was found.

Using thermal-expansion data for PZT from Fig. 2 and the thermal expansion of the substrate material Si,<sup>12</sup> Eq. (2) was used to calculate the thermal stress in a PZT film deposited on silicon as a function of temperature. These calculated thermal stress curves can then be compared with the experimental curve in Fig. 7. This thermal stress calculation was performed for three cases:

- The material in the film is randomly oriented and the thermal-expansion coefficient is  $\alpha_{\text{PZT}}$  [which equals  $(2\alpha_1 + \alpha_3)/3$ ].
- The polarization of the thin-film material is directed parallel to the substrate plane. The thermal expansion of the film parallel to the substrate is then given by  $(\alpha_1 + \alpha_3)/2$ .
- The polarization is directed perpendicularly to the substrate and the thermal expansion in the film parallel to the substrate is equal to  $\alpha_1$ .

From Fig. 7 it is clear that the experimentally determined curve of the thermal stress during thermal cycling of the PZT film is qualitatively much more similar to that calculated for case (b) than for the two other cases. These results strongly suggest that the crystallites within the PZT films grown as described above have a polarization with a large component directed in the plane of the film.

At 450 °C the tensile thermal stress reaches a maximum and above 450 °C it decreases. This indicates that above 450 °C the thermal expansion of the PZT in the plane of the film becomes higher than that of the Si substrate. As Fig. 2 shows, for bulk PZT this crossover point occurs at a temperature close to  $T_c$ .<sup>13</sup> So, if it is assumed<sup>17</sup> that the temperature at which the maximum in the stress occurs approximately corresponds to the Curie point,  $T_c$  is substantially higher than what has been found for the bulk material with  $T_c = 386$  °C.<sup>13</sup> A comparable increase of  $T_c$  has been observed by Kwok and Desu.<sup>17</sup> They attributed this increase to the intrinsic tensile stress, which was also observed in this study. This tensile stress shifts the volume-decreasing ferroelectric to paraelectric transition, i.e., the Curie point, to a higher temperature.<sup>17</sup> For  $\text{PbTiO}_3$  the pressure dependence of the Curie point for hydrostatic pressure is  $-0.07$  K/MPa as determined by Samara.<sup>18</sup> Assuming the same value holds for thin-film PZT material with a tensile stress in the plane of the film, for a tensile stress of 330 MPa at temperatures of around 400 °C the increase in  $T_c$  would amount to 23 °C. In view of the large number of assumptions, it can be concluded that this is a value not too far from the shift in  $T_c$  observed by us.

### C. Stress in the Pt top electrode

The as-deposited top electrode has a compressive stress ( $\sigma = -520$  MPa). This value is smaller than the value for the bottom electrode and it could indicate a somewhat changed microstructure. Figure 8 shows that thermal cycling of the top electrode shows a behavior very similar to that observed for the bottom electrode. It has to be noted that any changes in the stress of the PZT film are also included in the shape of the curves in Fig. 8. The stress in the top electrode at room temperature changed to 940 MPa tensile after a short anneal-

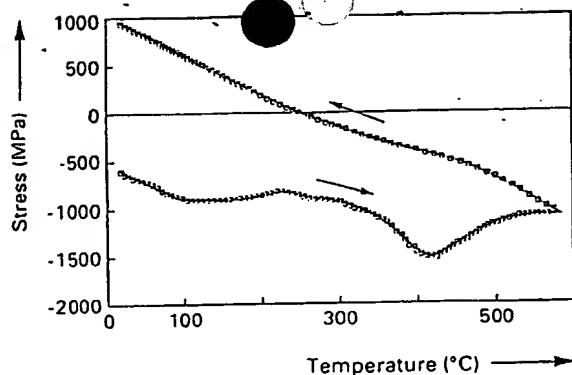


FIG. 8. Stress in a 70 nm Pt+7 nm Ti film sputtered on a 220 nm PZT film during a thermal cycle in  $N_2$ .

ing treatment (5 mins in  $O_2$  at 500 °C). This is again very similar to the values found for the bottom electrode after the temperature cycling in  $N_2$  as well as the annealing in  $N_2/O_2$  (Fig. 5). Such an annealing treatment of processed, i.e., structured ferroelectric capacitors, is found to give a substantial improvement of the electrical properties.<sup>8</sup>

#### IV. STRESS ANALYSIS BY REMOVAL OF CAPACITOR LAYERS

The total stress in the completed capacitor stack is the sum of the stresses in each film. When the stress of a film is measured after each processing step, the effect of this step on all the underlying films is also included in the curvature. This can give rise to an erroneous interpretation of the measurements. In order to eliminate such effects, stress measurements were carried out in combination with removal of the different films. In that case the change in curvature of the wafer can be attributed to the stress present in the removed film. In Table III stress values obtained by the film removal method for the case of as-deposited as well as annealed top electrodes are given.

##### A. Stress in the bottom electrode after removing the top electrode and the PZT film

The stress in the bottom electrode has to be compared with the value of 950 MPa before PZT deposition. It can be concluded that the stress in the bottom electrode is hardly influenced by the subsequent deposition, annealing, and etching process steps carried out during the processing of the ferroelectric stack, provided it is annealed at a temperature at least equal to the maximal PZT and TE processing tempera-

BE への応力は、その後の加工工程でほとんど変化を受けない。

TABLE III. The stress in the films within a fully processed stack as determined by the film removal method for as-deposited and annealed top electrodes.

Film	As deposited (MPa)	After anneal of top electrode (MPa)
Top electrode	-530	930
PZT	80	-37
Bottom electrode	~900	895

TABLE IV. Wafer curvature (in  $1000 m^{-1}$ ) at room temperature of wafers after the different BE and PZT processing steps with bottom electrodes annealed at 450, 550, and 650 °C, respectively. The curvature of the wafer after the deposition of the bottom electrode is arbitrarily taken to be 0  $m^{-1}$ .

Process step	Wafer curvature ( $10^3 m^{-1}$ )		
	Annealing temperature (°C)		
	450	550	650
After BE deposition	0	0	0
After BE annealing	0.8	8.5	16.4
After PZT layer 1	5.5	9.7	14.7
After PZT layer 2	9.2	11.2	15.1
After PZT layer 3	12.1	13.3	16.6
After PZT annealing	16.9	18.1	19.1

tures. In the case in which the PZT is deposited on bottom electrodes that are annealed at 450 and 550 °C, two stress-related effects occur simultaneously: the stress in the PZT film develops while the heating process (up to 650 °C) results in stress modifications in the bottom electrode. Both processes lead to a change in the curvature of the wafer; however, this change cannot be assigned to either film. Table IV gives the curvatures during PZT processing for three bottom electrodes annealed at the temperatures 450 (with  $\sigma = -660$  MPa), 550 (with  $\sigma = 166$  MPa), and 650 °C (with  $\sigma = 940$  MPa). The results show that during deposition of the PZT with processing temperatures up to 650 °C the difference in curvature found after the anneal of the bottom electrode at different temperatures gradually decreases. After the PZT annealing only a small difference remains. This indicated that the reconstruction of the Pt film that changes the stress level takes place even if the Pt film is covered with PZT. After the removal of the PZT and the top electrode all three types of bottom electrodes have similar tensile stresses of 850–950 MPa.

##### B. Stress in the PZT film after removing the top electrode

Table III shows a significant difference for the PZT film between the stresses after removal of the as-deposited electrode and after removal of the annealed top electrode. A comparison with the value before the deposition of the top electrode ( $\sigma = 113$  MPa; see Table II) also clearly demonstrates the shift toward a more compressive stress of the PZT film induced by the top electrode annealing. One would expect this shift on the basis of the large tensile stress observed in both the bottom and top electrodes after annealing treatments. In order to further investigate the stress state of the PZT film as it is in the complete P/PZT/Pt stack, we measured the dependence of the stress on a thermal cycling from 25 to 575 °C after removal of the top electrode. This was done for the two cases of an as-deposited and an annealed top electrode. The results are shown in Fig. 9. In both cases the stresses during heating and cooling are different, with by far the largest change in the case of the annealed top electrode. The stress curves measured during cooling from 575 °C are in both cases qualitatively the same as the thermal stress observed for the thermal cycling of an as-deposited

上電極を引抜た後に、  
PZT は引縮した。

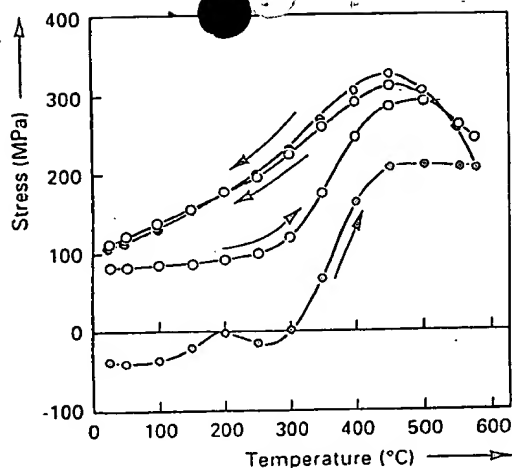


FIG. 9. Stress in a PZT film after deposition and etching of the top electrode. The film is thermally cycled to 575 °C with a heating rate of 15 °C/min. The stress development is shown for the case where the top electrode is not annealed (○) and annealed for 5 min at 500 °C in O<sub>2</sub> (●).

PZT film (Fig. 7). Thus the heat treatment of the PZT film without Pt on top restores the stress situation that was present before the deposition and annealing of the top electrode. In Sec. III B it was discussed that the direction of the polarization is then predominantly parallel to the substrate.

## V. ELECTRICAL RESULTS

We have investigated the switching properties of structured ferroelectric capacitors for the as-deposited and the annealed top electrode. In Fig. 10 the switched and nonswitched polarizations ( $\Delta P_s$  and  $\Delta P_{ns}$ ) are shown as functions of the pulse amplitude ( $V_p$ ). The measurements

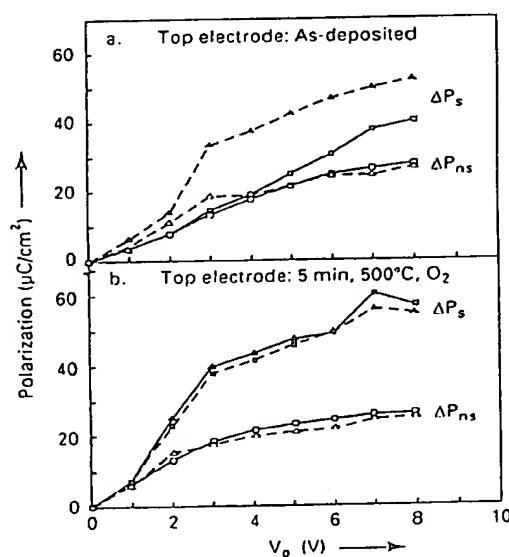


FIG. 10.  $\Delta P_s$  (filled symbols) and  $\Delta P_{ns}$  (open symbols) as functions of  $V_p$  for a 2000  $\mu\text{m}^2$  ferroelectric capacitor for a virgin capacitor (solid line) and after poling with 1000 pulses at 8 V (broken line) for as-deposited (upper panel) and for annealed (lower panel) top electrodes.

were done using single pulse switching and were carried out for the virgin capacitors ( $N=1$ ) and after poling with 1000 pulses at  $V_p=8$  V ( $N=1000$ ).

The unannealed capacitor shows a poor switching behavior for  $N=1$  with almost no difference between  $\Delta P_s$  and  $\Delta P_{ns}$  below 4 V and only a small difference above this voltage. It is seen that poling with 1000 pulses of 8 V greatly improves the switching behavior. For the annealed samples there is little difference between the curves for  $N=1$  and  $N=1000$ , i.e., the capacitor in its virgin state is easily switchable.

## VI. DISCUSSION AND CONCLUSIONS

A fully processed ferroelectric capacitor consists of a PZT film with a low compressive stress sandwiched between two platinum electrodes that both have a large thermal tensile stress of about 1 GPa (Table III). This stress situation is the result of the cumulative effect of the subsequent heat treatments applied during the processing of the Pt/PZT/Pt stack.

The as-deposited bottom and top electrodes both have an intrinsic compressive stress. An annealing treatment reduces the stress level, and after cooling to room temperature highly tensively stressed electrodes are obtained.

Annealing the bottom electrode prior to the sol-gel deposition of PZT is necessary in order to obtain a well-crystallized PZT. When the PZT is deposited on unannealed bottom electrodes, a poorly crystallized rosette-structured PZT film is obtained.<sup>19</sup> However, Table IV shows that the stress modification processes in the bottom electrode occur independently of the subsequent PZT and top electrode processing. Therefore, in any case, a bottom electrode with a thermal tensile stress of about 1 GPa is always obtained.

The three-layer PZT is under tensile stress after a final annealing at 650 °C. The stress in the PZT film is not influenced significantly by the deposition of the top electrode and remains tensile in nature.

The stress development in the PZT film during thermal cycling (Figs. 7 and 9) indicates that for the PZT films without a top electrode or with an as-deposited top electrode, a large fraction of the PZT crystallites have a large component of the polarization directed parallel to the plane of the substrate. This domain/crystallite orientation is essentially formed when the Curie point is passed while the PZT film is under tensile stress during cooling. It represents the energy minimum for PZT on top of a Pt electrode. This orientation is not changed when the top electrode is deposited at low temperatures.

The in-plane polar orientation might explain the observed switching behavior of the unannealed capacitors (Fig. 10). In the virgin state relatively few domains would be directed perpendicular to the substrate, and only after 1000 pulses of 8 V have a large fraction of the domains undergone a 90° reorientation. This tentatively explains the significant improvement of the switching behavior after 1000 pulses.

After the top electrode annealing, during which the PZT is heated to a temperature higher than the Curie point, the stress in the PZT at room temperature becomes compressive. After removal of the annealed top electrode the stress-

temperature curve of the PZT film shows a stress which is hardly influenced up to about 300 °C (Fig. 9). If this curve is compared with the calculated thermal stress curves for the polarization directed parallel or perpendicular to the surface of the substrate in Fig. 7, it is striking that the heating curve of Fig. 9 up to about 300 °C is qualitatively much more like the "perpendicular" curve than the "parallel" one. This strongly indicates that in the case of an annealed top electrode the direction of the polarization within the crystallites of the PZT film is largely directed perpendicular to the substrate. Presumably this is the result of the enclosure of the PZT film between two tensively stressed electrodes during the cooling process and while passing the Curie point which modifies the state of the polarization within the PZT film at which the total energy is minimized. The electrical switching behavior showing a high switchable polarization in a virgin state of the film is consistent with this orientation.

Turning back to Fig. 9 it is clear that for a PZT film which has been annealed with a top electrode on top and from which the top electrode has been removed, at temperatures above 300 °C there is a marked increase in tensile stress with temperature. This indicates that after the top electrode is removed and the PZT film is heated again some kind of domain reorientation occurs. On cooling this film again after heating to 575 °C the polarization is again directed parallel to the substrate which is a situation similar to that observed in the as-deposited films. This is clearly the state with minimal energy when there is no platinum electrode on top.

In conclusion, the switching properties of ferroelectric capacitors, in particular, of virgin capacitors, are improved by an annealing treatment due to a reorientation of the direction of the polarization from parallel to perpendicular to the

substrate. In this way fully functional capacitors can be obtained without the need for an additional poling treatment.

- <sup>1</sup> D. Berlincourt, J. Acoust. Soc. Am. 70, 1586 (1981).
- <sup>2</sup> H. H. A. Krueger, J. Acoust. Soc. Am. 42, 636 (1967); 43, 576 (1968); 43, 583 (1968).
- <sup>3</sup> J. A. Thornton and D. W. Hoffman, Thin Solid Films 117, 5 (1989).
- <sup>4</sup> S. B. Desu, J. Electrochem. Soc. 140, 2981 (1993).
- <sup>5</sup> B. A. Tuttle, J. A. Voigt, T. J. Garino, D. C. Goodnow, R. W. Schwartz, D. L. Lamppa, T. J. Headley, and M. O. Eatough, in *Proceedings of the IEEE 8th International Symposium on Applied Ferroelectrics* (IEEE, New York, 1992), pp. 344-348.
- <sup>6</sup> G. A. C. M. Spierings, J. van Zon, P. K. Larsen, and M. Klee, Integrated Ferroelectr. 3, 283 (1993).
- <sup>7</sup> M. Klee, R. Eusemann, R. Waser, and H. van Hal, J. Appl. Phys. 71, 1566 (1992).
- <sup>8</sup> G. J. M. Dormans, P. K. Larsen, G. A. C. M. Spierings, J. Dikken, M. J. E. Ulenaers, R. Cuppens, D. J. Taylor, and R. D. J. Verhaar, Integrated Ferroelectr. 6, 93 (1995).
- <sup>9</sup> J. J. van Glabbeek, G. A. C. M. Spierings, M. J. E. Ulenaers, G. J. M. Dormans, and P. K. Larsen, Mater. Res. Soc. Symp. Proc. 310, 127 (1993).
- <sup>10</sup> G. G. Stoney, Proc. R. Soc. London, Ser. A 82, 172 (1909).
- <sup>11</sup> L. Holborn and A. L. Day, Ann. Phys. 4, 104 (1901).
- <sup>12</sup> T. Soma and H.-M. Kagaya, in *Properties of Silicon* (Inspec, London, 1988), Chap. 1.12, pp. 33-34.
- <sup>13</sup> W. R. Cook, Jr., D. A. Berlincourt, and F. J. Scholz, J. Appl. Phys. 34, 1392 (1963).
- <sup>14</sup> J. A. Ruud, A. Witvrouw, and F. Spaepen, Mater. Res. Soc. Symp. Proc. 209, 737 (1990).
- <sup>15</sup> P. K. Larsen, R. Cuppens, and G. J. M. Dormans, Proceedings of the NATO Advanced Workshop on Science and Technology of Electroceramic Thin Films, Italy, 1994 (unpublished).
- <sup>16</sup> K. Sreenivas, I. Reaney, T. Maerder, N. Setter, C. Jagadish, and R. G. Elliman, J. Appl. Phys. 75, 232 (1994).
- <sup>17</sup> C. K. Kwok and S. D. Desu, Mater. Res. Soc. Symp. Proc. 310, 429 (1993).
- <sup>18</sup> G. A. Samara, Ferroelectrics 2, 227 (1971).
- <sup>19</sup> G. A. C. M. Spierings, M. J. E. Ulenaers, G. L. M. Kampschöer, H. A. M. van Hal, and P. K. Larsen, J. Appl. Phys. 70, 2290 (1991).